

Magnetic resonance in the noncollinear hexagonal antiferromagnets CsNiCl_3 and CsMnBr_3

I. A. Zaliznyak, L. A. Prozorova, and S. V. Petrov

Institute of Physics Problems, USSR Academy of Sciences
(Submitted 27 July 1989)

Zh. Eksp. Teor. Fiz. **97**, 359–366 (January 1990)

Antiferromagnetic resonance is investigated in the compounds CsNiCl_3 and CsMnBr_3 , which have a triangular antiferromagnetic ordering at $T < T_N$. The measurements were carried out at frequencies 0.6–180 GHz in fields up to 58 kOe. All the relativistic oscillation modes were investigated in the easy-axis antiferromagnet CsNiCl_3 . It is shown that the $\nu_i(H)$ dependence is described by the spin-wave theory equations. The exchange integral in the hexagonal plane J' and the effective anisotropy constant \bar{D} were found to equal 8 and -0.59 GHz, respectively. The theoretical relation $\nu_1 \propto H^3$ is confirmed for the zero-gap mode of the easy-plane antiferromagnet CsMnBr_3 , for which one of the exchange modes was investigated and the constants $J' = 0.50$ GHz and $\bar{D} = 1.95$ GHz were obtained.

1. INTRODUCTION

The crystal structure of most halide compounds ABX_3 (A is an alkali metal, B is a divalent metal of the $3d$ group) is described by the symmetry group D_{6h}^4 and its unit cell contains two formula units.¹ The ions A and X form in this structure a hexagonal close packed lattice, and the ions of the $3d$ metals B are located inside octahedra of the halide ions. These octahedra, with abutting faces, form columns elongated along the C_6 axis (Fig. 1a). The packing of most known compounds of this type is ideal (the octahedra in the columns are not distorted) and as a result the ratio of the lattice constants is $c/a = (2/3)^{1/2} = 0.816$.

This crystal structure imparts to these compounds specific magnetic properties.² The most important is quasi-one-dimensionality: the exchange integral J indicative of the interaction between the magnetic ions arranged along the C_6 axis and spaced $c/2$ apart exceeds by two or three orders the exchange J' in the basal plane via the indirect exchange B–X–X–B (Fig. 1b). The magnetic system can therefore be regarded as an aggregate of weakly coupled linear, in our case antiferromagnetic, chains stretched along the hexagonal axis.

It is convenient to express the spin Hamiltonian of the system in the form

$$\mathcal{H} = J \sum_{i,j} \mathbf{S}_i \cdot \mathbf{S}_j + J' \sum_{i,j}'' \mathbf{S}_i \cdot \mathbf{S}_j + D \sum_i (S_i^z)^2 - \gamma H \sum_i S_i^z \quad (1)$$

The first term describes here exchange interaction along the chain, the second exchange in the basal plane, and the third and fourth the anisotropy energy and the Zeeman energy of the spins in the external field H . In the compounds CsNiCl_3 and CsMnBr_3 considered in the present paper, the spin interaction is antiferromagnetic: $J > 0$, $J' > 0$.

Below the Néel temperature determined by the value of $(JJ')^{1/2}$, the atomic spins are ordered into a three-dimensional noncollinear antiferromagnetic structure described in the general case by six sublattices. According to the neutron-diffraction and NMR data,^{3–5} a planar triangular “120-degree” structure is realized in these magnets in the absence of a field, viz., all the spins are coplanar and so oriented that the angle between neighbors in the basal plane is close to 120° , while neighboring spins along the hexagonal axis are

antiparallel. The fact that the experimentally determined magnetic structure is close to helicoidal with a propagation vector $\mathbf{Q} = (1/3, 1/3, 1)$, which is realized at $T = 0$ when account is taken of only the exchange (antiferromagnetic) interaction, attests to the smallness of the relativistic effects. The latter, however, determine the orientation of the spins relative to the crystal axes.

In CsNiCl_3 the anisotropy constant is $D < 0$ and the anisotropic interactions tend to align the spins with the hexagonal axis. The equilibrium configuration in this case is such that every third spin in the basal plane is oriented along the C_6 axis, while its neighbors deviate from it by angles close to $\pm 120^\circ$ (Fig. 2a). Just as in an ordinary collinear easy-axis antiferromagnet, a magnetic field applied along the C_6 axis produces, when the critical field value H_c is reached, a spin-flop transition in which the spins become reoriented and end up practically in the basal plane.

In CsMnBr_3 ($D > 0$) the spins lie in the basal plane of the crystal (Fig. 2b). The anisotropy in this substance exceeds the weak exchange in the plane ($D > J'$). If the external field is directed along the C_6 axis, the hexagonality of the magnetic structure does not lead to singularities: the spins are rotated in a magnetic field towards the axis, and the transverse spin components form as before a 120-degree structure up to the spin-flip transition. If, however, the field

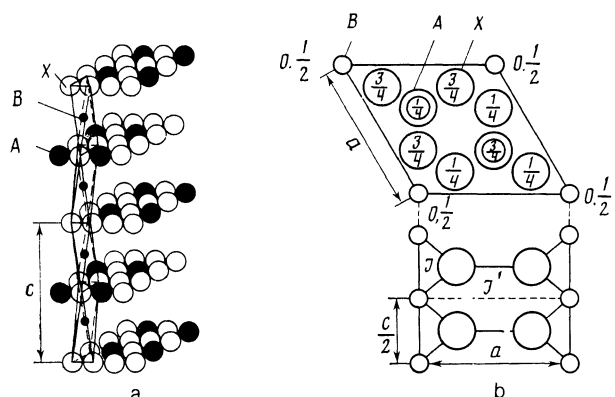


FIG. 1. Crystal structure of CsNiCl_3 type (a) and arrangement of the atoms in a unit cell of the CsNiCl_3 (b). The numbers denote the coordinates of the atoms.

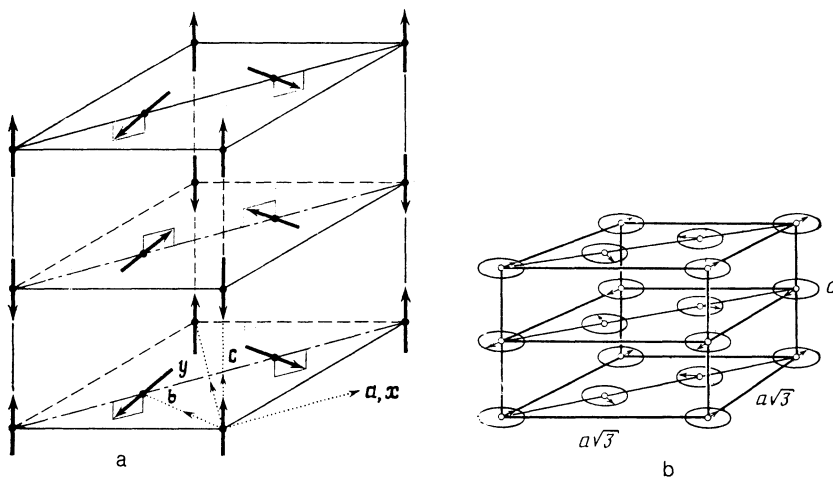


FIG. 2. Magnetic structures of CsNiCl_3 (a) and CsMnBr_3 (b).

is applied in the basal plane, competition between the anisotropy and the weak exchange sets in: the anisotropy tends to preserve the spin directions in the plane, while the exchange J' tends to set them perpendicular to the applied field. As shown in Ref. 6, hexagonality plays in this case the principal role: in contrast to a two-sublattice antiferromagnet, the reorientation is accompanied here by a second-order phase transition. According to calculation, when a field $\mathbf{H} \perp C_6$ is applied the spins of the sublattices remain in the basal plane. In weak fields, the spins of one pair of sublattices are set almost perpendicular to the field ($\alpha \approx \mp \pi/2$), while those of the two other pairs are set at angles $\beta \approx \pm \pi/6$ and $\gamma \approx \pm 5\pi/6$. As the field is increased, the angles α and $\beta + \gamma$ vary little, and the angle $\beta - \gamma$ decreases in accordance with a definite law and vanishes in the critical field H_c , i.e., pairwise collapse of the four sublattices takes place. The succeeding reorientation proceeds in standard fashion: when the field is increased the angles α and β decrease and vanish in the spin-flip transition field. The existence of a field with collapsed sublattices in CsMnBr_3 was recently proved by neutron diffraction.⁷

The frequencies of the antiferromagnetic resonance in the described magnetic structures were calculated by Marchenko and Chubukov.^{6,8,9} The present paper reports an experimental investigation of the resonance properties of CsNiCl_3 and CsMnBr_3 .

2. SAMPLES AND EXPERIMENT

The measurements were made on single-crystal samples produced in the following manner.

CsNiCl_3 . The substance was synthesized in the form of a fine-crystalline well-filtered brown precipitate by mixing hot CsCl and NiCl_2 solutions in concentrated hydrochloric acid. The dried filtered precipitate was placed in a quartz ampul which was subsequently evacuated for 5 hours at a temperature gradually rising to 300°C . The ampul was next sealed off and moved by a clockwork mechanism, at a speed 1 mm/h, through an oven heated to 800°C . The single crystal produced in this ampul was annealed in a muffle furnace at $500\text{--}600^\circ\text{C}$ for 10 days. The crystals were transparent, dark-red, and cleanly cleaved along a binary plane.

CsMnBr_3 . MnBr_2 was synthesized by interaction of MnCO_3 with hydrobromic acid. The resultant solution was evaporated dry on a water bath. The precipitated crystals

were dried for a week in a vacuum desiccator over granulated KOH and placed in a quartz ampul, to which a stoichiometric amount of CsBr was added. The mixture of the salts was evacuated with a forevacuum pump at a temperature $200\text{--}300^\circ\text{C}$ for several days. The ampul was then sealed and moved by a clockwork mechanism at a speed 1 mm/h through a furnace heated to 600°C . The crystals were annealed in the same ampul at 400°C for 10 days. The resultant single crystals were likewise transparent, dark pink, with a cleavage plane coinciding with a binary plane. The CsMnBr_3 crystals were quite hygroscopic and had to be handled with some caution, otherwise they became completely degraded after three or four months.

The agreement between the crystal structure of the produced substances and the structures of CsNiCl_3 and CsMnBr_3 was confirmed by x-ray phase analysis. The single crystal samples were parallelepipeds with linear dimensions 1–2 mm. The crystallographic axes were also oriented by x-ray diffraction.

To check on the $\nu(H)$ functional dependences and to determine the constants that enter in the Hamiltonian, measurements were needed in a wide range of frequencies ν and of static magnetic fields H . We used for this purpose several direct-amplification microwave spectrometers covering the range from 0.6 to 180 GHz. A static magnetic field up to 59 kOe was produced by a superconducting solenoid. The absorbing cells were high- Q cavities of various constructions, with a short-circuited waveguide serving as the absorbing cell in the upper part of the frequency band. The investigated samples were secured at the antinode of the microwave magnetic field with rubber cement.

The resonant absorption was determined from the change of the amplitude P of a microwave signal of constant frequency passing through the cell with the sample while the static magnetic field was smoothly varied. The $P(H)$ dependence was recorded with an x - y plotter.

The sample temperature was measured with a semiconductor resistance thermometer.

3. EXPERIMENTAL RESULTS AND THEIR DISCUSSION

CsNiCl_3 . Resonance absorption was observed at $T > T_N = 4.7\text{ K}$ in the form of a single line of width $\Delta H = 1\text{--}2\text{ kOe}$. The relation between the frequency and the field is

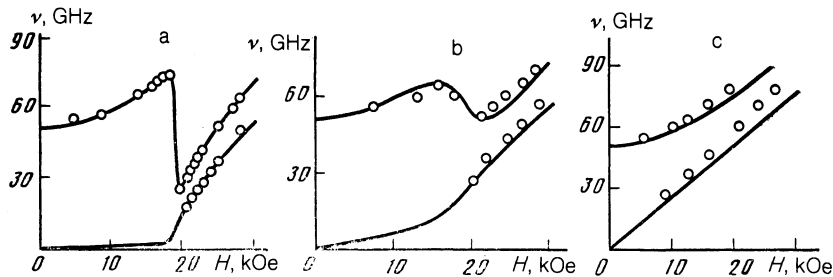


FIG. 3. Antiferromagnetic resonance spectrum in CsNiCl_3 at $T = 1.7$ K. The theoretical curves and the experimental data are given for various angles between the field direction and the C_6 axis: a) $\varphi = 1^\circ$; b) $\varphi = 10^\circ$, c) $\varphi = 90^\circ$.

here $\nu = \gamma H$, where $\gamma = 3.0 \pm 0.1$ GHz/kOe, in agreement with the data of Ref. 2.

A complicated resonance-frequency spectrum is observed at $T < T_N$. Near T_N the lines are very broad ($\Delta H \sim 10$ kOe). The main investigations were made at $T = 1.7$ K. The experimental results are shown in Figs. 3 and 4.

The resonance frequencies were calculated on the basis of a microscopic model in Ref. 8. The spectrum consists of 6 modes. Three are due to exchange and their frequencies in weak fields are

$$\nu_{4,5} = 3 \cdot 2^{1/2} (JJ')^{1/2}, \quad \nu_6 = 12 (JJ')^{1/2},$$

and three are relativistic, whose frequencies at $\mathbf{H} \parallel C_6$ take different forms at $H < H_c$ and $H > H_c$, where H_c is the spin-flop transition field. For $H < H_c$

$$\nu_1 = \gamma (\eta H_c^2 + H^2)^{1/2},$$

$$\nu_2 = \gamma (H_c/2 \cdot 3^{1/2}) (\tilde{D}/J') [1 - (H/H_c)^2]^{1/2}, \quad \nu_3 = 0,$$

and for $H > H_c$

$$\nu_{1,2} = \gamma \left\{ \left[\left(\frac{1+\eta}{2} \right)^2 H^2 - \eta H_c^2 \right]^{1/2} \pm \frac{1-\eta}{2} H \right\}, \quad \nu_3 = 0,$$

where

$$H_c^2 = 16 \tilde{D} J S^2 \left(1 + \frac{9}{4} \frac{J'}{J} \right) \left(1 + \frac{9}{8} \frac{J'}{J} \right),$$

$$\eta = \frac{\chi_\perp - \chi_\parallel}{\chi_\parallel} = \left(1 + \frac{9}{4} \frac{J'}{J} \right)^{-1}, \quad \tilde{D} = D \left(1 - \frac{1}{2S} \right).$$

These equations agree in general outline with the results

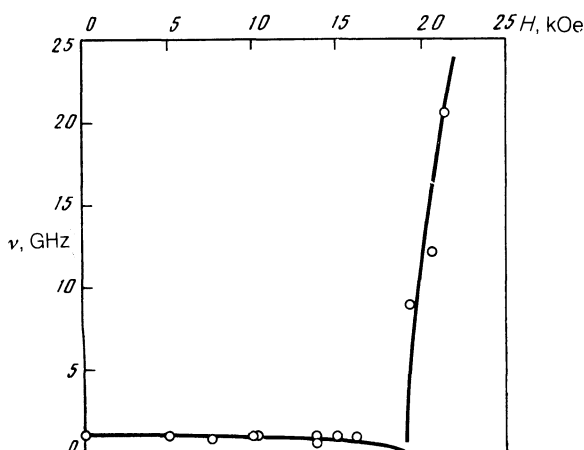


FIG. 4. Low-frequency part of the CsNiCl_3 spectrum at $T = 1.7$ K, $\mathbf{H} \parallel C_6$.

of a macroscopic calculation,⁹ so that the macro- and microscopic parameters at $T = 0$ could be related. The only difference between Eqs. (2) and the macroscopic-calculation results is that allowance for terms of higher order in the anisotropy constant led at $H < H_c$ to a nonzero resonance frequency ν_2 for the mode connected with rotation in the spin plane.

Figure 3 show results of an AFMR investigations at 20–80 GHz and $T = 1.7$ K. These data are well described by the theoretical equations for $\nu_1(H)$ and $\nu_2(H)$ if the constants are $\gamma = 3.0$ GHz/kOe, $H_c = 19.2$ kOe, and $\eta = 0.8$.

The difficulty of experimentally observing the ν_2 mode in fields $H < H_c$ was due to the need for very exactly setting the crystal easy axis C_6 parallel to the field, for even a one-degree deflection makes the $\nu_2(H)$ dependence practically nondispersive. We have observed in the experiments a very broad absorption line with $\Delta H \sim 10$ kOe, most strongly pronounced at 0.8 GHz. The line vanished completely below 0.6 GHz, but was shifted towards weaker field when the frequency was raised, decreased in amplitude, and also vanishes at ≈ 1.2 GHz. In view of the large width of the observed resonance-absorption line, it can be assumed that it corresponds just to the weakly dispersive $\nu_2(H)$ mode (see Fig. 4). The value of $\nu_2(0) = \nu_2(H=0)$ estimated from experiment is 1.1 GHz.

These results differ substantially from the experimental data of Ref. 10, where resonance absorption was observed at 8.8 and 20 GHz for $\mathbf{H} \parallel C_6$ and ascribed by the authors to the resonance mode $\nu_2(H)$ at $H < H_c$. We have undertaken searches for this resonance absorption but obtained no positive results.

Knowledge of the two relativistic frequencies at $H = 0$, viz. $\nu_2(0) = 1.1$ GHz and $\nu_1(0) = 53$ GHz, as well as of the exchange integral $J = 345$ GHz determined with good accuracy from neutron-diffraction investigations of resonance frequencies on half the Brillouin zone,¹¹ makes it possible to obtain the respective values $J' = 8$ GHz $\pm 10\%$ and $\tilde{D} = -0.59$ GHz $\pm 10\%$ of the exchange integral in the basal plane and the anisotropy constant.

Note that we are speaking of quantities that determine the long-wave dynamics of the system. They can differ significantly from the true microscopic spin-Hamiltonian parameters because of the zero-point oscillations. It is important, however, that the quantum renormalizations do not alter the functional dependences of the relativistic frequencies²: Eqs. (2) contain the same values of J , J' and \tilde{D} renormalized to the experimental zero-point oscillations.

Using our results, we can calculate the frequencies of the exchange modes $\nu_{4,5,6}$ and compare them with the neutron-diffraction data.^{11,13} Substituting our data in Eqs. (2) we obtain $\nu_6 = 575$ GHz and $\nu_{4,5} = 407$ GHz. A mode of

frequency 520 Hz, close to our estimate of ν_6 , was obtained in Refs. 11 and 13. In Ref. 11, furthermore, a mode with a gap $\nu_0 = 220$ GHz was obtained in a zero field and was initially interpreted there as the ν_1 mode. In our opinion this interpretation is incorrect, since it follows from our experiments that the ν_1 mode has a gap at 53 GHz (see Fig. 3): the size of the gap corresponds to the flopping field H_c , and the field dependence of the resonance frequency is well described by the theoretical equations. It is not excluded that the $\nu_0 = 220$ GHz oscillation corresponds to one of the exchange modes ν_4 or ν_5 . A quantitative explanation of the substantial decrease of the resonance frequency ν_0 compared with that predicted by the theory for $\nu_{4,5} = \nu_6/2^{1/2}$, as well as the discrepancy between the experimental and theoretical values of ν_6 , requires a detailed theoretical analysis. It is possible that this discrepancy is the result of effects due to zero-point oscillations that are made strong by the quasi-one-dimensionality of the substance, inasmuch as according to Haldane's prediction¹⁴ an antiferromagnet with $S = 1$ remains paramagnetic also at $T = 0$ in the one-dimensional case. Haldane's effect is not realized in CsNiCl_3 in pure form, since a finite T_N exists, but inasmuch as the estimated gap between the ground (singlet) and first-excited states in a one-dimensional ferromagnet, $\nu \approx 0.8$, $J = 280$ GHz¹⁵ agrees approximately with the frequencies of the exchange modes, one should expect the zero-point oscillations to lower these frequencies substantially, and the renormalization affects to the greatest degree just the modes $\nu_{4,5}$. Another possible explanation of the presence of a resonance mode with a gap $\nu_0 \sim 220$ GHz was recently proposed by Affleck.¹⁶

CsMnBr₃. A study of equilibrium configurations of spins in CsMnBr_3 and a calculation of the resonance frequencies are reported in Ref. 6. The spectrum, just as in CsNiCl_3 , consists of six modes: three relativistic and three exchange. Since, however, $\tilde{D} > J'$ in this substance, the two exchange modes ν_4 and ν_5 in weak magnetic fields lie below the relativistic ν_3 and ν_2 .

Of greatest interest is the spectrum at $\mathbf{H} \perp C_6$ because at this external-field orientation a reorientation of the spins takes place in the easy plane and is accompanied by a phase transition corresponding to the collapse of two pairs of sublattices. This transition takes place in a field $H_c = (48JJ'S^2)^{1/2}$.

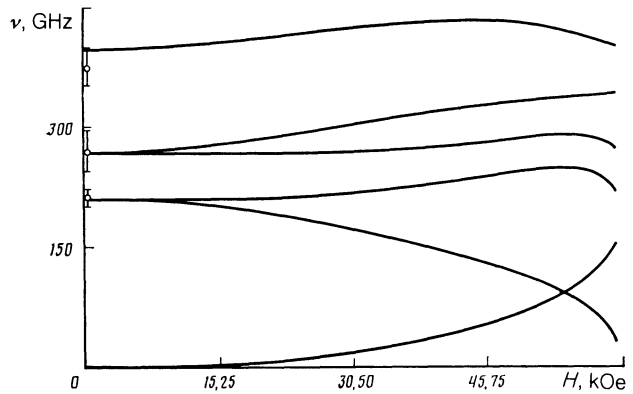


FIG. 5. Calculation of the antiferromagnetic-resonance spectrum for CsMnBr_3 using the equations of Ref. 6 and the constants of Ref. 17 for $\mathbf{H} \perp C_6$. Points—experimental data from Ref. 17.

The dependence of the resonance frequencies on the magnetic field is described by cumbersome expressions that can simplify substantially only at $H = 0$ and $H = \tilde{H}_c$.

Figure 5 shows results of an actual calculation, using the equations of Ref. 6, of the antiferromagnetic-resonance spectrum in CsMnBr_3 . The constants of J , J' , and \tilde{D} were taken from Ref. 17. As seen from Fig. 5, the band investigated by us contains ν_1 and ν_5 , i.e., one relativistic and one exchange mode.

Two resonance absorption lines were observed in Ref. 5 for $T < T_N = 8.3$ K and $\mathbf{H} \perp C_6$. The widths of the low- and high-frequency lines were $\Delta H \sim 1 - 3$ and $\Delta H \sim 2 - 3$ kOe. The results of experiments performed at $T = 1.7$ K are shown in Fig. 6. Since the resonance absorption was measured at $T \ll T_N$, the temperature-induced changes of the spectrum can be disregarded, and the equations of Ref. 6 can be used for the calculations. According to the theory, the first antiferromagnetic-resonance mode $\nu_1(H)$ has no energy gap at $H = 0$. The theoretical $\nu_1(H)$ dependence is not trivial, for $\nu_1 \propto H^3$ in weak fields. For the exchange mode ν_5 the theory yields at $H = 0$ an $\nu_5(H)$ dependence in the form $\nu_5 = \tilde{H}_c (3/2)^{1/2}$. As the field is increased, the frequency ν_5 decreases monotonically and vanishes at a second-order phase transition point (for $H = \tilde{H}_c$). Our experimental data agree well with these functional relations. The best agree-

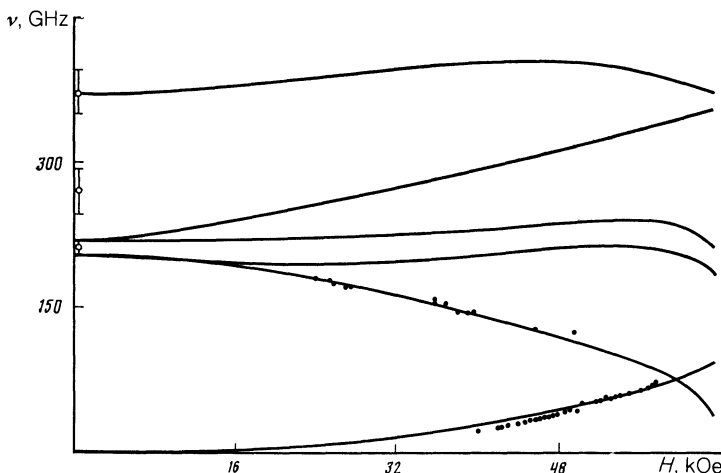


FIG. 6. Antiferromagnetic-resonance spectrum in CsMnBr_3 : ●—Results of our experiment at $T = 1.7$ K, $\mathbf{H} \perp C_6$; ○—experimental data of Ref. 17, lines—theoretical calculation using the equations of Ref. 6 with the constants $\gamma = 2.8$ GHz/kOe, $J = 214$ GHz, $J' = 0.5$ GHz, $\tilde{D} = 1.05$ GHz.

ment is obtained for the following values of the constants:

$$\begin{aligned}\gamma &= 2.8 \text{ GHz/kOe}, J = 214 \text{ GHz (taken from Ref. 17)}, \\ J' &= 0.5 \text{ GHz} \pm 5\%, \tilde{D} = 1.95 \text{ GHz} \pm 5\%.\end{aligned}$$

The results of the calculation of the total antiferromagnetic resonance spectrum with these constants are shown by the solid lines in Fig. 6. Our values of J' and \tilde{D} differ somewhat from the data obtained using inelastic neutron scattering,¹⁷ namely $J' = 0.46 \text{ GHz}$ and $\tilde{D} = 2.9 \text{ GHz}$. The experimental points of Ref. 17 are also shown in Fig. 6. It can be seen that in the case of CsMnBr_3 all the experimental results agree well with the theoretical calculations.

The authors thank A. S. Borovik-Romanov for interest in the work, V. I. Marchenko and A. V. Chubukov for helpful discussions, and B. Ya. Kotyuzhanskii for valuable remarks.

¹K. S. Aleksandrov, A. T. Anistarkhov, B. V. Beznosikov, and N. V. Fedoseeva, in *Phase Transitions in Crystals of ABX_3 Halide Compounds* [in Russian], Nauka, Novosibirsk, 1981, p. 264.

- ²N. Achiba, *J. Phys. Soc. Jpn.* **27**, 561 (1969).
³W. B. Yelon and D. E. Cox, *Phys. Rev. B* **6**, 204 (1972); **7**, 2024 (1973).
⁴R. H. Clark and W. G. Moulton, *ibid.* **B 5**, 788 (1972).
⁵M. Eibschutz, R. C. Sherwood, F. S. L. Hsu, and D. E. Cox, *AIP Conf. Proc.* **17**, 864 (1972).
⁶A. V. Chubukov, *J. Phys. C* **21**, 441 (1988).
⁷V. D. Gaulin, T. E. Mason, M. F. Collins, and J. Z. Larese, *Phys. Rev. Lett.* **62**, 1380 (1989).
⁸I. A. Zalisnyak, L. A. Prozorova, and A. V. Chubukov, *J. Phys.* **1**, 4743 (1989).
⁹I. A. Zalisnyak, V. I. Marchenko, S. V. Petrov, *et al.*, *Pis'ma Zh. Eksp. Teor. Fiz.* **47**, 172 (1988) [*JETP Lett.* **47**, 211 (1988)].
¹⁰H. Tanaka, S. Teraoka, E. Kakekashi, *et al.*, *J. Phys. Soc. Jpn.* **57**, 1153 (1988).
¹¹W. J. L. Buyers, R. M. Morra, R. L. Armstrong, *et al.*, *Phys. Rev. Lett.* **56**, 371 (1986).
¹²A. F. Andreev and V. I. Marchenko, *Usp. Fiz. Nauk* **132**, 39 (1980) [*Sov. Phys. Usp.* **23**, 21 (1980)].
¹³R. M. Morra, W. J. L. Buyers, R. L. Armstrong, and K. Hirakawa, *Phys. Rev. B* **38**, 543 (1988).
¹⁴F. D. M. Haldane, *Phys. Rev. Lett.* **50**, 1153 (1983).
¹⁵J. C. Bonner and G. Muller, *Phys. Rev. B* **29**, 3216 (1983).
¹⁶I. Affleck, *Phys. Rev. Lett.* **62**, 474 (1989).
¹⁷B. D. Gaulin, M. F. Collins, and W. J. L. Buyers, *J. Appl. Phys.* **61**, 3409 (1987).

Translated by J. G. Adashko